



# Microelectromechanical disk resonators for direct detection of liquid-phase analytes

Emad Mehdizadeh <sup>a,\*</sup>, Jennifer C. Chapin <sup>b</sup>, Jonathan M. Gonzales <sup>c</sup>, Amir Rahafrooz <sup>a</sup>, Reza Abdolvand <sup>c</sup>, Byron W. Purse <sup>b,2</sup>, Siavash Pourkamali <sup>a,1</sup>

<sup>a</sup> Department of Electrical and Computer Engineering, University of Denver, Denver, CO 80208, USA

<sup>b</sup> Department of Chemistry and Biochemistry, University of Denver, Denver, CO 80208, USA

<sup>c</sup> School of Electrical and Computer Engineering, Oklahoma State University, Stillwater, OK 74078, USA

## ARTICLE INFO

### Article history:

Received 23 January 2014

Received in revised form 5 May 2014

Accepted 19 May 2014

Available online 2 June 2014

## ABSTRACT

This paper presents preliminary measurement results for real-time detection of biomolecules using rotational-mode MEMS resonant structures and capability of such to directly and specifically measure concentration of thiol-terminated DNA molecules in liquid. Thin film piezoelectric disk resonators with quality factors ( $Q$ ) as high as  $\sim 100$  in aqueous solutions have been fabricated and utilized as direct biomolecular detectors that can address the problem of low  $Q$  for MEMS resonators when in direct contact with liquid. To adsorb thiol-terminated molecules, a gold layer is deposited on the top resonator surface. A gradual frequency shift of  $\sim 10$  kHz (3800 ppm) was recorded in real-time while forming monolayers of mercaptohexanol in aqueous solution, demonstrating the potential of such structures as highly sensitive biosensors. Over and above detection of target single-stranded-DNA (ssDNA) sequences using the disk resonators (with mass sensitivities as high as  $19.3 \text{ ppm cm}^2/\text{ng}$  ( $65 \text{ Hz cm}^2/\text{ng}$ ) in aqueous solution), the response of such devices has been characterized using different concentrations of thiol-terminated DNA molecules. For one order of magnitude change in concentration of functionalizing thiol-terminated-ssDNA solution,  $\sim 2X$  difference in measured frequency shifts of the disk resonators was observed.

© 2014 Elsevier B.V. All rights reserved.

## 1. Introduction

Detection and measurement of liquid-phase analytes is essential in various biomedical and biotechnology applications [1]. Biochemical changes in the patient's body fluids can signal organ damage or dysfunction in advance, prior to observable microscopic cellular damages or other symptoms [2]. Moreover, early, rapid, and sensitive detection of most diseases is vital for successful clinical treatment. Majority of the currently available biosensing and bioanalysis platforms, such as diagnostics chips are based on fluorescent labeling and optical detection methods [3–9]. Optical detection requires relatively sophisticated and bulky readout

components including light sources, CCD cameras, lenses, etc. The complex and time consuming sample preparation procedures including extra steps for fluorescent labeling is another disadvantage of this approach. Furthermore, such techniques normally only produce the end result of biomolecular reactions and do not provide real-time information on the kinetics of the reaction, which is very important in many cases including drug development and drug delivery research. While a great deal of research is being devoted to miniaturization of optical readout apparatus [10,11] and facilitating fluorescent labeling processes [12,13], compact label-free biosensors with electrical readout and real-time measurement capability could offer a shortcut towards improved disease diagnostics and theranostics at lower cost [14].

Electromechanical resonant microbalances such as Quartz Crystal Microbalances (QCMs) [15–17] or surface acoustic wave (SAW) sensors [18,19] are capable of label-free molecular detection by direct real-time monitoring of the added mass to their surfaces. However, such devices also have relatively large sizes and cannot compete with fluorescent microarrays in terms of throughput. In many cases their sensitivity is not adequate either. Microelectromechanical resonant structures are, on the other hand,

\* Corresponding author. Current address: Electrical Engineering Department, University of Texas at Dallas, Richardson, TX 75080, USA. Tel.: +1 720 224 4714.

E-mail address: [emad.mehdizadeh@utdallas.edu](mailto:emad.mehdizadeh@utdallas.edu) (E. Mehdizadeh).

<sup>1</sup> Current address: Electrical Engineering Department, University of Texas at Dallas, Richardson, TX 75080, USA.

<sup>2</sup> Current address: The Department of Chemistry and Biochemistry, San Diego State University, San Diego, CA 92182, USA.

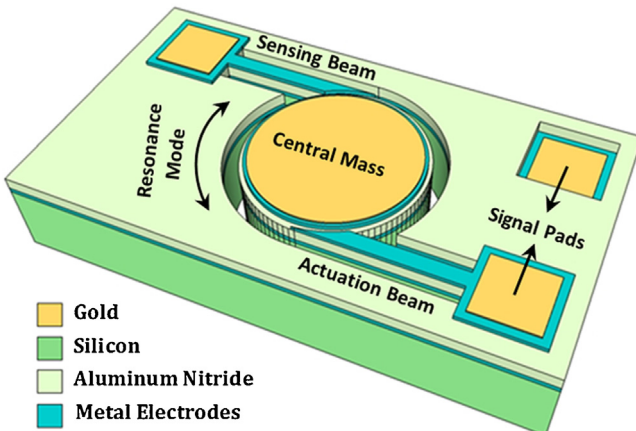


**Fig. 1.** Schematic view of the gold-coated TPoS rotational-mode disk resonant structures.

smaller and more sensitive integrated versions of the same devices capable of real-time biomolecular sensing with large throughputs [20–24]. The resonance frequency shift caused by added molecular mass on the resonator surface can be used to detect and measure smallest concentrations of liquid-phase analytes. When it comes to biomedical applications, however, such devices are usually dominated with excessive viscous forces in liquid media. Consequently, most of formerly reported MEMS resonant devices cannot usually operate in liquid or only show very low quality factors while the quality factor of resonating sensing platforms in the target environment plays a significant role in their frequency stability and in turn the attainable mass resolutions. Although shown as highly sensitive biosensors, high-frequency thermal-piezoresistive MEMS resonators are not capable of operating in liquid and the frequency measurements need to be carried out in air after different reaction steps [22]. Film-bulk-acoustic-resonators (FBARs) used as direct real-time biosensors, only show Q-factors as small as 15 when in contact with liquid [23]. In another work Qs up to 189 were achieved using a contour-mode ring-shape FBAR by only having the top surface of the resonator in contact with aqueous solution [24]. With only one beam, such resonators are not also robust enough for many applications. To realize higher Q-factors in liquid, thermal-piezoresistive disk resonators were demonstrated with Qs up to ~300 in liquid [25]. Operating in their rotational mode, the resonators' surfaces only slide in parallel to the fluid-solid interface minimizing the effect of fluid viscous damping on the devices as well as the energy loss into the liquid. The heat generated by thermal actuation in such devices, however, can adversely impact the molecular interactions. To overcome this problem, similar disk resonant devices were realized using TPoS technology showing Qs up to ~100 in liquid [26,27]. Coated with gold on the top surface (see Fig. 1), the same resonators are utilized here for direct in-liquid detection of thiol-terminated molecules as well as distinguishing between matched and mismatched DNA strands. Since detection ability alone is not adequate for a biosensing platform, concentration measurement capability is also demonstrated using such devices.

## 2. Resonator fabrication and description

A TPoS, Thin-film Piezoelectric on Substrate, resonant structure comprises a thin piezoelectric film (e.g. aluminum nitride) sandwiched between two metallic electrodes (e.g. Molybdenum) all stacked on top of the device layer of a silicon-on-insulator (SOI) substrate (Fig. 2a) [28]. The top metal layer is dry etched in ICP to form the top electrodes and the signal pads while the aluminum

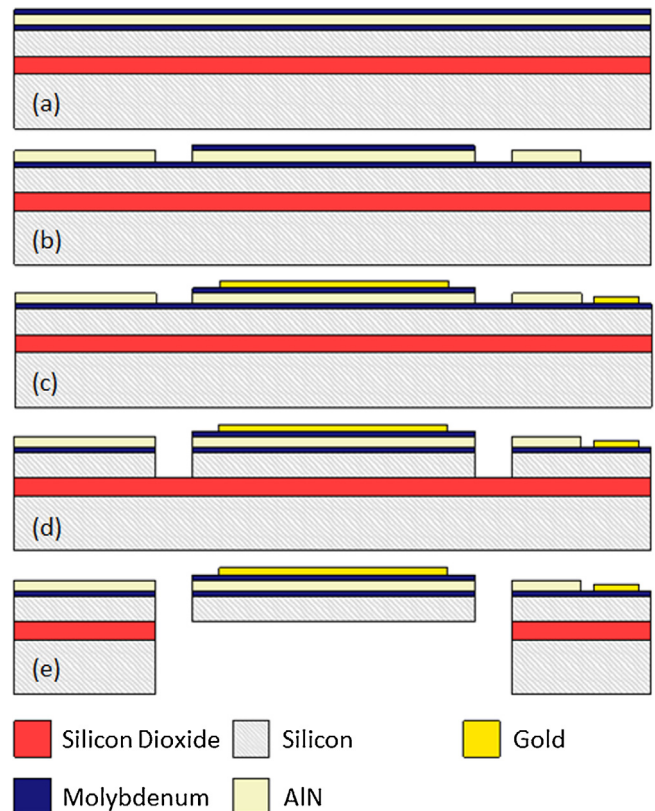


**Fig. 2.** Process flow for TPoS resonators starting with (a) thin-film stack deposition of Mo/AlN/Mo; (b) top metal dry etch in ICP followed by AlN wet etch in hot TMAH to access bottom metal; (c) gold layer deposition and patterning; (d) bottom metal dry etch followed by silicon device layer anisotropic dry etch in DRIE; (e) silicon handle layer anisotropic dry etch in DRIE followed by silicon dioxide wet etch release.

nitride (AlN) is wet etched in hot TMAH to access the bottom metal layer (Fig. 2b). After e-beam evaporation and patterning a 1000 Å thick layer of gold (Fig. 2c), the resonator body is defined in a stack dry etch step (Fig. 2d). The backside silicon handle layer is then etched in an anisotropic etching step followed by removing SOI buried oxide layer in hydrofluoric acid (HF), leaving free-standing structures behind (Fig. 2e).

A scanning electron microscopic image of a ~3.4 MHz piezoelectric disk resonator implemented via the TPoS platform is depicted in Fig. 3. The fabricated disk resonator structure consists of a circular central mass and two support beams. Metal coated AlN films on the support beams are responsible for actuation and sensing of the resonant device. Upon application of an ac voltage at the resonance

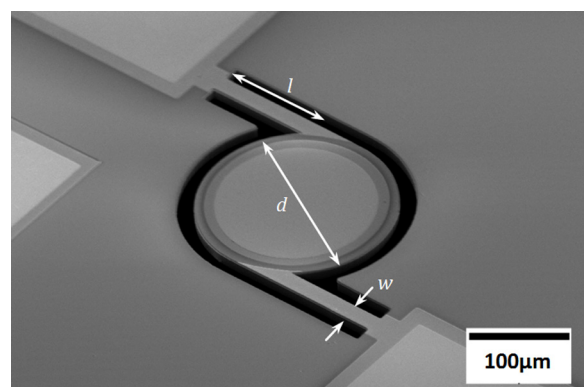


**Fig. 3.** Scanning electron microscope view of a ~3.4 MHz thin-film piezoelectric on silicon (TPoS) rotational mode disk resonator.

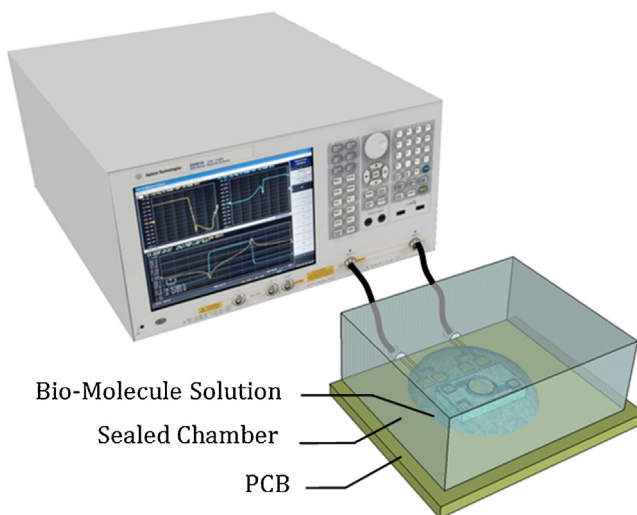


**Fig. 4.** Schematic view of the experimental setup.

frequency of the structure to the top metal electrode on one of the support beams, the support beams start vibrating in their longitudinal mode resulting in rotational mode vibration of the disk. The electric charge generated by the resulting stress/strain in the other support beam due to the piezoelectric effect is then harvested from the output electrode. The gold, as an inert and biocompatible material, on top of the disk allows modification of the resonator surface with thiol-terminated molecules.

### 3. Experiments and results

To maintain the solution concentrations unchanged throughout the experiments i.e. prevent persistent evaporation of the buffer solutions into the surroundings, a setup was prepared (see Fig. 4) in which a very small sealed chamber, comprised of a glass cap with clay as the sealant, is responsible for creating a water saturated enclosed environment.

Treating the disk resonators with aqueous solution of 6-Mercapto-1-Hexanol (briefly referred to as mercaptohexanol or MCH), their resonance frequency was monitored using an Agilent E5061B network analyzer over time. MCH,  $\text{HSCH}_2(\text{CH}_2)_4\text{CH}_2\text{OH}$ , is a thiol compound used in proteomics research both as a spacer thiol and a model biomolecule containing a carbon-bonded sulphydryl group (SH). Such molecules bond tightly to Au-coated surfaces through the sulphydryl functional group, creating very robust surface-covalent gold-sulfur bonds [29]. As MCH molecules bond to the resonator surface over time, the resonance frequency of the resonator decays exponentially (see Fig. 5), as expected from kinetics of self-assembled monolayer formation [30], reaching saturation after about 1 h. A gradual shift of ~3800 ppm in agreement with the kinetics of the molecular interactions at the solid–liquid interface clearly demonstrates promising performance of such resonant devices on direct in-liquid mass monitoring of analytes in real-time with very high sensitivities.

Three 65-mer oligonucleotide probes purchased from Integrated DNA Technologies (IDT), shown in Table 1, were used in another set of experiments. The 65-mer nucleotide probe of entry 1 is a thiol-terminated ssDNA (HS-ssDNA) molecule used for immobilization on the Au-coated surface of the resonators through the thiol-group at the 5'-end. The single-stranded probe of entry 2, which is the complement of that of entry 1, is used for the hybridization purpose. Whereas the 65-mer oligonucleotide sequence of entry 3 is a mismatched DNA strand used for the validation purpose.

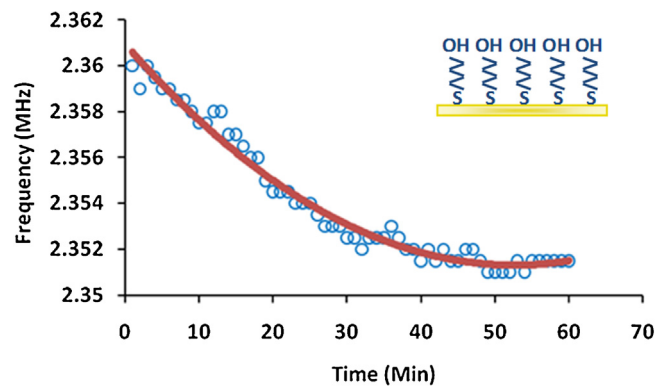


**Fig. 5.** The recorded frequency of a disk resonator ( $d = 200$ ,  $w = 16$ ,  $l = 160$ ,  $t = 15$ ) during exposure to MCH Solution.

To realize maximum hybridization of the two complements, the gold-coated surfaces were treated with HS-ssDNA (2.0 M/1.0 M  $\text{KH}_2\text{PO}_4$ , pH 4.2) for 2 h followed by 1 h of post-treatment in MCH (1.0 mM in aqueous solution) to form a mixed-monolayer. A primary advantage of using the two-step process to form HS-ssDNA/MCH mixed monolayers is that nonspecifically adsorbed DNA is largely removed from the surface. Thus, the majority of available ssDNA probes on the surface give rise to specific hybridization with complementary oligonucleotides discriminating between complementary and noncomplementary target molecules. In effect, MCH can form strong gold-thiolate bonds with the surface replacing the nonspecific bonds between negatively charged ssDNA and resonator surface. The number of HS-ssDNA probes immobilized on the surface as a result of such mixed surface treatments would be  $\sim 5.7 \times 10^{12}$  molecules/cm<sup>2</sup> [31]. Treating the functionalized surface with 1.0  $\mu\text{M}$  complementary DNA in 1.0 NaCl-Tris-HCl-1.0 mM EDTA, pH 7.5,  $\sim 100\%$  hybridization is then attainable [31]. The schematic of the surface treatments is briefly illustrated in Fig. 6.

Due to the conductive nature of the two buffer solutions in functionalization and hybridization steps and lack of an insulation layer on the device metallic electrodes, at this point the resonance frequencies for those steps were not monitored in real-time. Instead, the frequency responses were recorded in distilled water once the devices were completely rinsed after each treatment step (see Fig. 7). The measurement results for two resonators with different dimensions, summarized in Table 2 as well as Fig. 8, show close to 2 times higher sensitivity (ppm cm<sup>2</sup>/ng) for device 2 with bigger plate size (smaller resonance frequency). After the hybridization step, the frequency shift of 12.5 kHz (3700 ppm) was obtained from the second device which corresponds to a mass loading of 192.1 ng/cm<sup>2</sup> resulting in a sensitivity of 19.3 ppm cm<sup>2</sup>/ng (65 Hz cm<sup>2</sup>/ng), showing  $\sim 28X$  better sensitivity than that of the-state-of-the-art FBARs (0.7 ppm cm<sup>2</sup>/ng) when operating in liquid [24]. If the resonators are interfaced with sustaining amplifiers forming self-sustained oscillators, the minimum detectable frequency change is related to the short-term frequency instability of the resonance frequency. The standard measure of short-term frequency instabilities in the

**Table 1**  
DNA sequences used in the experiments.

Entry	Sequence
(1)	5'-(HS-C <sub>6</sub> )-CA GGA GTG TCA ACG CCA ATA TTC TCC TAG CCT GCA CAG ACA GTC GTG CTC TAC TAT GAC AAG GTT-3'
(2)	5'-AAC CTT GTC ATA GTA GAG CAC GAC TGT CTG TGC AGG CTA GGA GAA TAT TGG CGT TGA CAC TCC TG-3'
(3)	5'-TGT ATA TTG CTC TCA CAT GAA CAA ATT AGT AGA GTG CCG CTT TCA GCC CCC CTG TCG TCG GCG AC-3'

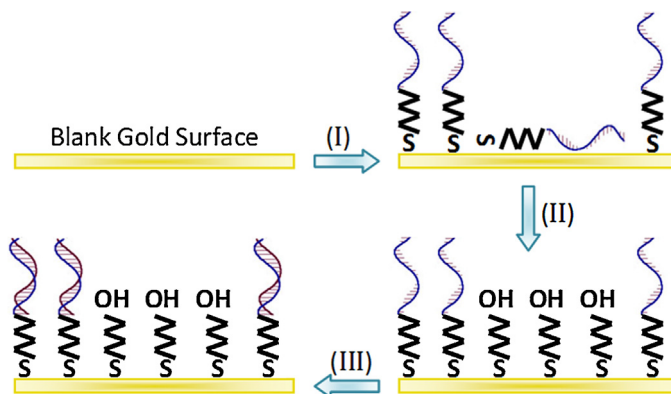


**Fig. 6.** Schematic of surface functionalization and complementary DNA hybridization. (I) Exposure to HS-ssDNA ( $2.0 \mu\text{M}/1.0 \text{ M KH}_2\text{PO}_4$ , pH 4.2) for 2 h; a portion of ssDNA molecules are nonspecifically adsorbed to the surface. (II) Treatment with  $1.0 \text{ mM}$  Mercapto-Hexanol aqueous solution for 1 h for removing nonspecific portion of adsorbed HS-ssDNA probes. (III) Hybridization with target ssDNA solution ( $1.0 \mu\text{M}/1.0 \text{ M NaCl-Tris-HCl-1.0 \text{ mM EDTA}$ , pH 7.5) for 30 min.

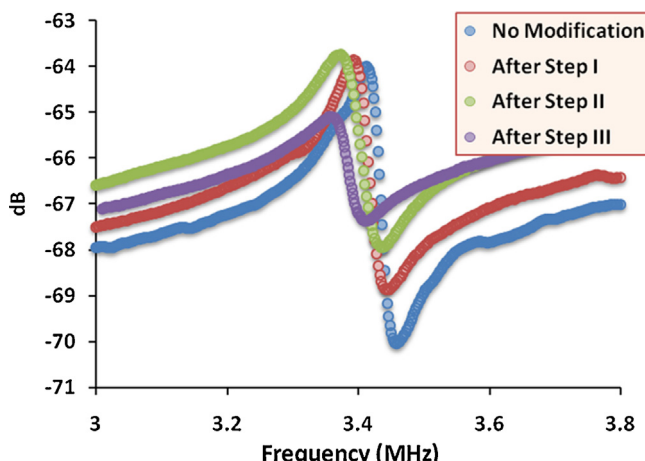


**Fig. 7.** Recorded frequency responses for the  $\sim 3.4 \text{ MHz}$  disk resonator of Fig. 3 ( $d = 200$ ,  $w = 16$ ,  $l = 100$ ) in distilled water after different treatment steps.

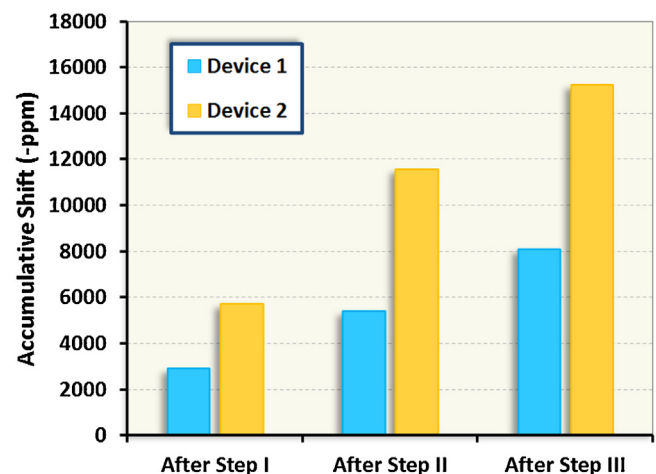


**Fig. 8.** Accumulative ppm frequency shifts obtained for two devices listed in Table 2 after different treatment steps shown in Fig. 6.

time domain, commonly referred to as noise, is called Allan deviation  $\sigma_y(\tau)$  [32]. Within the sampling time of  $\sim 0.1\text{--}10 \text{ s}$ , which is the typical region where the frequency of resonant sensors is measured, Allan deviation is minimum and can be empirically calculated as  $\sigma_y(\tau) = 1.0 \times 10^{-7}/Q$  [33]. Accordingly, the minimum detectable frequency deviation would be equal to  $f_0 \times \sigma_y(\tau)$ , where  $f_0$  is the resonance frequency of the resonator, resulting in values as low as  $0.007 \text{ Hz}$  ( $\sigma_y(\tau) = 2.5 \times 10^{-9}$ ) for resonators in the present work. However, to count for practical issues such as temperature fluctuations, a conservative frequency measurement resolution of  $0.7 \text{ Hz}$  is used here resulting in a mass resolution of  $11 \text{ pg/cm}^2$ . Applying the same approach to the-state-of-the-art FBARs [24], a mass resolution of  $76 \text{ pg/cm}^2$  is attained which suggests  $\sim 7$ -fold improvement by the TPOs disk resonators.

It should however be noted that if appropriate protocols are not rigorously followed in label-free detection procedures, false responses as a result of non-specific adsorption will be inevitable. Therefore, to rule out any prospect of irrelevant frequency shifts two separate experiments are conducted here. First, several devices only treated with MCH were immersed in complementary DNA solution and no shift was observed after 1 h exposure. The same result was acquired when a functionalized sample was exposed to the solution of mismatched DNA probes for 1 h. It is therefore

**Table 2**

Summary of measurement results obtained from piezoelectric disk resonant devices in distilled water after different modification steps shown in Fig. 6.

Device#	Dimensions ( $\mu\text{m}$ )	Quality Factor	Frequency (MHz)	Accumulative Shift (ppm)
(1)	$d=100$ $w=8$ $l=70$ Device Layer (DL)=5	48	6.0225	-
		Step I		
		32	6.0050	-2906
		Step II		
		24	5.9900	-5396
		Step III		
		19	5.9737	-8103
		54	3.4120	-
		Step I		
		43	3.3925	-5715
	$d=200$ $w=16$ $l=100$ DL=5	Step II		
		39	3.3725	-11577
		Hybridization with <u>Mismatched</u> DNA Solution		
		38	3.3725	-11577
		Step III		
		27	3.3600	-15240

} Validation via  
Mismatched  
DNA

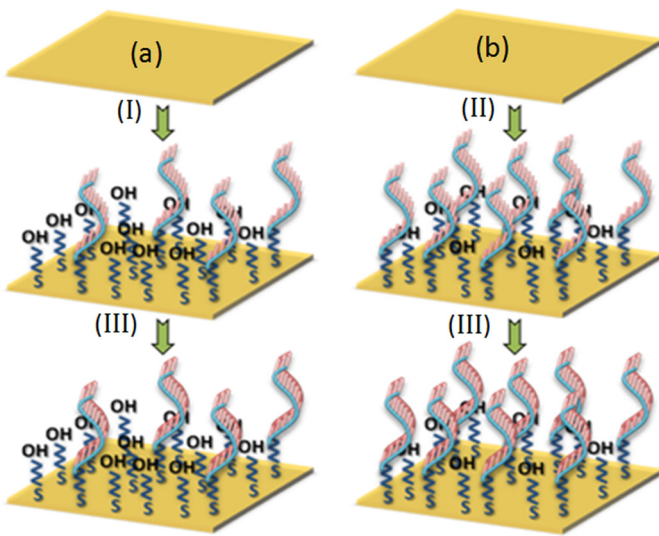


**Fig. 9.** Schematic of the characterization experiments for concentration measurements (I) Exposure to 1.0  $\mu\text{M}$  [0.1% HS-ssDNA, 99.9% MCH] for 15 min. (II) Exposure to 1.0  $\mu\text{M}$  [1% HS-ssDNA, 99% MCH] for 15 min. (III) Hybridization with complementary ssDNA solution (1.0  $\mu\text{M}$ /1.0 M NaCl Tris-HCl-1.0 mM EDTA) for 30 min.

inferred that the frequency shifts are caused by specific hybridization with complementary nucleotides.

Since the detection ability alone is not inadequate for a biosensing platform, the concentration measurement capability of the TPoS disk resonant sensors is also investigated. In order to characterize the effect of different concentrations of biomolecules on the sensor responses, the TPoS disk resonators were exposed to mixed solutions with different ratios of mercaptohexanol and thiol-terminated ssDNA molecules. The schematic of biomolecular events in the designed experiments is shown in Fig. 9. The thiol-terminated ssDNA and MCH molecules compete for bonding to the available gold atoms on the resonator surface. As expected, due to the higher mass of DNA molecules than MCH, the total frequency shift observed increased as the concentration ratio of thiol-terminated DNA to MCH increased. Two identical MEMS chips each containing several resonators with different dimensions were

treated with different ratios of MCH and thiol-terminated ssDNA molecules. The two sets of resonators were treated with 1.0  $\mu\text{M}$  [0.1% HS-ssDNA, 99.9% MCH] and 1.0  $\mu\text{M}$  [1% HS-ssDNA, 99% MCH] both in 1.0 M KH<sub>2</sub>PO<sub>4</sub>, pH 4.2 each for 15 min. The ppm shifts obtained after exposure to the higher concentration of HS-ssDNA were ~2–3 times as large in the aqueous solution. Almost the same trend was observed after hybridization of the same functionalized resonators with the complementary DNA sequence, 1.0  $\mu\text{M}$ /1.0 M NaCl Tris-HCl-1.0 mM EDTA, pH 7.5. After this step, the ppm shifts observed were 6–7 times as large for the sample functionalized with higher concentration of HS-ssDNA molecules. This is well expected as in such samples a larger number of HS-ssDNA molecules, immobilized on the resonator surface, are present to hybridize with target molecules. Table 3 summarizes the measurement results for the two sets of resonators. The results confirm a clear and consistent correlation between the functionalizing DNA concentrations and response of similar rotational mode disk resonators.

#### 4. Conclusions

Gold coated rotational-mode disk resonant devices were introduced as highly sensitive mass balances for direct liquid-phase measurements of biosamples. Due to minimal viscous damping while operating in liquid media, such structures could be used as reliable tools for real-time monitoring of biomolecular interactions. Qs as high as 100 were obtained for such devices when operating in aqueous solutions. Direct liquid-phase monitoring of frequency, while forming monolayers of MCH, was performed in real-time that well matches the kinetics of molecular interactions at the solid–liquid interface. Direct in-liquid detection of target ssDNA strands was also demonstrated showing frequency shifts as large as ~3000 ppm. To investigate the ability of the biomolecular sensors for concentration measurements, the resonators were exposed to matching target ssDNA solution after functionalization with thiol-terminated ssDNA (HS-ssDNA) solutions with different concentrations. The results exhibit a ~2X difference in measured frequency shifts for one order of magnitude change in concentration of functionalizing HS-ssDNA solution. Future work includes providing electrical insulation for the

**Table 3**

Summary of measurement results obtained from the resonant structures in distilled water after different treatment steps illustrated in Fig. 8.

Dimensions ( $\mu\text{m}$ )	Chip # 1			Chip # 2			Shift Ratio
	Frequency	Shift (ppm)	Q Factor	Frequency	Shift (ppm)	Q Factor	
$d=500$ $l=340$ $w=40$ $t = 5$	1.0883	-	92	1.0895	-	93	-
	15 min exposure to 1.0 $\mu\text{M}$ [1% DNA, 99% MCH]			15 min exposure to 1.0 $\mu\text{M}$ [0.1% DNA, 99.9% MCH]			
	1.0853	-2757	72	1.0884	-1010	90	2.7
	20 min exposure to 1.0 $\mu\text{M}$ Complementary DNA solution			20 min exposure to 1.0 $\mu\text{M}$ Complementary DNA solution			
$d=500$ $l=240$ $w=40$ $t = 5$	1.0793	-5512	58	1.0875	-825	82	6.7
	1.2500	-	82	1.2470	-	38	-
	15 min exposure to 1.0 $\mu\text{M}$ [1% DNA, 99% MCH]			15 min exposure to 1.0 $\mu\text{M}$ [0.1% DNA, 99.9% MCH]			
	1.2471	-2320	76	1.2455	-1203	28	1.9
20 min exposure to 1.0 $\mu\text{M}$ Complementary DNA solution				20 min exposure to 1.0 $\mu\text{M}$ Complementary DNA solution			
1.2413	-4650	38	1.2445	-802	22	5.8	

resonator electrodes to enable real-time monitoring of the resonance frequency in conductive buffer solutions. Interfacing the TPoS disk resonators with sustaining amplifiers, implementation of arrays of individually functionalized resonators, and integration of such devices within microfluidic channels are among tasks required to demonstrate a powerful biosensing platform using this technology.

## Acknowledgments

This research was supported by the State of Colorado Office of Economic Development and University of Denver.

## References

- [1] M.M. Elrick, J.L. Walgren, M.D. Mitchell, D.C. Thompson, Proteomics: recent applications and new technologies, *Basic Clin. Pharmacol. Toxicol.* 98 (2006) 432–441.
- [2] C.H. Ahn, J.W. Choi, G. Beauchage, J.H. Nevin, J.B. Lee, A. Puntambekar, J.Y. Lee, Disposable smart lab on a chip for point-of-care clinical diagnostics, *Proc. IEEE* 92 (2004) 154–173.
- [3] J. Homola, S.S. Yee, G. Gauglitz, Surface plasmon resonance sensors: review, *Sens. Actuators B: Chem.* 54 (1999) 3–15.
- [4] B. Cunningham, P. Li, B. Lin, J. Pepper, Colorimetric resonant reflection as a direct biochemical assay technique, *Sens. Actuators B: Chem.* 81 (2002) 316–328.
- [5] F. Vollmer, S. Arnold, Whispering-gallery-mode biosensing: label-free detection down to single molecules, *Nat. Methods* 5 (2008) 591–596.
- [6] C.R. Taitt, G.P. Anderson, F.S. Ligler, Evanescent wave fluorescence biosensors, *Biosens. Bioelectron.* 20 (2005) 2470–2487.
- [7] A. Leung, P.M. Shankar, R. Mutharasan, A review of fiber-optic biosensors, *Sens. Actuators B: Chem.* 125 (2007) 688–703.
- [8] L. Su, W. Jia, C. Hou, Y. Lei, Microbial biosensors: a review, *Biosens. Bioelectron.* 26 (2011) 1788–1799.
- [9] K. Yamana, Y. Ohtani, H. Nakano, I. Saito, Bis-pyrene labeled DNA aptamer as an intelligent fluorescent biosensor, *Bioorg. Med. Chem. Lett.* 13 (2003) 3429–3431.
- [10] J.R. Wojciechowski, et al., Organic photodiodes for biosensor miniaturization, *Anal. Chem.* 81 (2009) 3455–3461.
- [11] M. Nordstrom, D.A. Zauner, M. Calleja, J. Hubner, A. Boisen, Integrated optical readout for miniaturization of cantilever-based sensor system, *Appl. Phys. Lett.* 91 (2007) 103512.
- [12] H.B. Hsieh, et al., High speed detection of circulating tumor cells, *Biosens. Bioelectron.* 21 (2006) 1893–1899.
- [13] B.A. Flusberg, High-speed, miniaturized fluorescence microscopy in freely moving mice, *Nat. Methods* 5 (2008) 935–938.
- [14] A. Sassolas, B.D. Leca-Bouvier, L.J. Blum, DNA biosensors and microarrays, *Chem. Rev.* 108 (2008) 109–139.
- [15] C.K. O'Sullivan, G.G. Guilbault, Commercial quartz crystal microbalances – theory and applications, *Biosens. Bioelectron.* 14 (1999) 663–670.
- [16] S.H. Lee, D.D. Stubbs, J. Cairney, W.D. Hunt, Rapid detection of bacterial spores using a quartz crystal microbalance (QCM) immunoassay, *IEEE Sens. J.* 5 (2005) 737–743.
- [17] I.D. Avramov, A 0-phase circuit for QCM-based measurements in highly viscous liquid environments, *IEEE Sens. J.* 5 (2005) 425–432.
- [18] I. Mannelli, M. Minunni, S. Tombelli, M. Mascini, Bulk acoustic wave affinity biosensor for genetically modified organisms detection, *IEEE Sens. J.* 3 (2003) 369–375.
- [19] K. Lange, B.E. Rapp, M. Rapp, Surface acoustic wave biosensors: a review, *Anal. Bioanal. Chem.* 391 (2008) 1509–1519.
- [20] R. McKendry, J. Zhang, Y. Arntz, T. Strunz, M. Hegner, H.P. Lang, M.K. Baller, U. Certa, E. Meyer, H.J. Guntherodt, C. Gerber, Multiple label-free biodetection and quantitative DNA-binding assays on a nanomechanical cantilever array, *Proc. Natl. Acad. Sci. U.S.A.* 99 (2002) 9783–9788.
- [21] W. Pang, H. Zhao, E.S. Kim, H. Zhang, H. Yu, X. Hu, Piezoelectric microelectromechanical resonant sensors for chemical and biological detection, *Lab Chip* 12 (2012) 29–44.
- [22] B. Tousifar, S. Pourkamali, M. Kvasnika, B.W. Purse, Surface functionalization and monolayer formation on silicon resonant nanoballances, in: *Proc. Joint IFCS/EFTF Conf.*, 2011, pp. 1–5.
- [23] H. Zhang, M.S. Marma, S.K. Bahi, E.S. Kim, C.E. McKenna, Sequence specific label-free DNA sensing using film-bulk-acoustic-resonators, *IEEE Sens. J.* 7 (2007) 1587–1588.
- [24] W. Xu, S. Choi, J. Chae, A contour-mode film bulk acoustic resonator of high quality factor in a liquid environment for biosensing applications, *Appl. Phys. Lett.* 96 (2010) 053703.
- [25] A. Rahafrooz, S. Pourkamali, Rotational mode disk resonators for high-Q operation in liquid, in: *Proc. IEEE Sens. Conf.*, 2010, pp. 1071–1074.
- [26] E. Mehdizadeh, J. Gonzales, A. Rahafrooz, R. Abdolvand, S. Pourkamali, Piezoelectric rotational mode disk resonators for liquid viscosity monitoring, *Tech. Dig. Hilton Head Workshop* 35 (2012) 359–362.
- [27] E. Mehdizadeh, J. Chapin, J. Gonzales, A. Rahafrooz, B. Purse, R. Abdolvand, S. Pourkamali, Direct detection of biomolecules in liquid media using piezoelectric rotational mode disk resonators, *Proc. IEEE Sens. Conf.* (2012) 1–4.
- [28] R. Abdolvand, H.M. Lavasani, G. Ho, F. Ayazi, Thin-film piezoelectric-on-silicon resonators for high-frequency reference oscillator applications, *IEEE Trans. Ultrason. Ferroelectr. Freq. Control* 55 (2008) 2596–2606.
- [29] H. Häkkinen, The gold–sulfur interface at the nanoscale, *Nat. Chem.* 4 (2012) 443–455.
- [30] D.K. Schwartz, Mechanisms and kinetics of self-assembled monolayer formation, *Annu. Rev. Phys. Chem.* 52 (2001) 107–137.
- [31] T.M. Herne, M.J. Tarlov, Characterization of DNA probes immobilized on gold surfaces, *J. Am. Chem. Soc.* 119 (1997) 8916–8920.
- [32] D.W. Allan, J.A. Barnes, A modified Allan variance with increased oscillator characterization ability, in: *Proc. 35th Annual Frequency Control Symposium*, 1981, pp. 470–475.
- [33] J.R. Vig, F.L. Walls, A review of sensor sensitivity and stability, *Proc. IEEE/EIA IFCs* (2000) 30–33.